

Scientific paper

# Monodispersed Gold Nanoparticles as a Probe for the Detection of Hg<sup>2+</sup> Ions in Water

## Bindhu Muthunadar Rajam,<sup>1</sup> Parimaladevi Ramasamy<sup>2</sup> and Umadevi Mahalingam<sup>2,\*</sup>

<sup>1</sup> Department of Physics, Nanjil Catholic College of Arts and Science, Nedumcode, Kaliyakavilai-695502, Tamil Nadu, India

<sup>2</sup> Department of Physics, Mother Teresa Women's University, Kodaikanal-624101, Tamil Nadu, India

\* Corresponding author: E-mail: ums10@yahoo.com Tele: 04542241685 (UM and PR)

Received: 08-11-2016

#### **Abstract**

Gold nanoparticles were synthesized using *Ananas comosus* as reducing agent. UV-visible spectra show the surface plasmon resonance peak at 544 nm. TEM measurement shows that the formation of monodispersed spherical nanoparticles with average size of 7 nm. Crystalline nature of the nanoparticles was evident from TEM images and peaks in the XRD pattern. FTIR analysis provides the presence of biomolecules responsible for the reduction and capping of the prepared gold nanoparticles. A selective and sensitive method is proposed for detecting mercury based on the SPR change of gold nanoparticles. This mercury sensor based on surface plasmon optical sensor can be used in water analysis.

Keywords: Ananas comosus. gold nanoparticles, mercury, optical sensor

#### 1. Introduction

The determination of heavy metal ions in water is of great importance because of their role in the physiological functions of biological systems. 1 Among the heavy metal ions, mercury is an most dangerous metal ions for environment and has most commonly toxic risks for human contacting areas as a result of natural processes, because it is widely distributed in air, water and soil and it is a toxic element that exists in metallic, inorganic, and organic forms.<sup>2</sup> Mercuric ion (Hg<sup>2+</sup>), exists mostly in surface water due to its high water solubility and it can cause several developmental delays and health problems that can damage the brain, nervous system, kidneys, and endocrine system.<sup>3,4</sup> Therefore, the analysis and measurement of detecting mercury in aqueous media is important. A variety of methods have been developed for quantification of Hg<sup>2+</sup> concentrations such as atomic absorption spectroscopy, inductive coupled plasma mass spectroscopy, electrochemical impedance spectroscopy, voltammetry and polarography. But, these methods are expensive, complicated sample treatment and mostly take a long measuring period. The selective optical sensor is an alternative method and has been attracted due to the excellent sensitivity, rapid response, the ability to do the detection in a non-destructive manner and cost-effective.

Metal nanoparticles have been received much attention due to their unique optical, electrical and catalytic properties. The size, shape and surface morphology of the particles were crucial in tuning these properties of nanosized metal particles. This was mostly significant for noble metals having strong surface plasmon resonance (SPR) oscillations. There were many synthetic methods have been developed to prepare nanoparticles, including chemical, physical and biological methods, among which green synthesis of metal nanoparticles remains the simplest and environment friendly method. All these synthetic methods vary generally in the way the electrons required for the reduction were provided. Green synthesis of nanoparticles using D.carota, S.lycopersicums, Beetroot, H. Cannabinus leaf, Moringa oliefera flower, Avena sativa and Hibiscus cannabinus stem has been reported. 5-11 Among the different metallic nanoparticles, gold nanoparticles have diverse activities and exhibit novel properties such as high surface and variation in electronic and optoelectronic properties; have made them more appropriate for therapeutic use and broad applications in nanobiotechnology. The chemical inertness and resistance to surface oxidation make gold an important material for use in nanoscale technologies and devices. This property is crucial when particle size approaches the nanostructure and the dominance of surface atoms results in an enhanced chemical reactivity.

In this work, gold nanoparticles were synthesized using *Ananas comosus* fruit extract as reducing agent. Since *Ananas comosus* is a readily available fruit and it is a good source of water, carbohydrates, sugars, vitamins A, C and carotene, beta. <sup>12</sup> It contains low amounts of protein, fat, ash and fibre. It is a good source of citric acid, malic acid and ascorbic acid <sup>12,13</sup> and also contain three types of amino acids. Along with this, it also contains bromelain, a protein-digesting enzyme that reduces inflammation. Modified pineapple peel fibre was used to remove heavy metal ions in water through the reaction with succinic acid anhydride. <sup>14,15</sup> Bhosale *et al.* reported the synthesis of nanoparticles using *Ananas comosus* extract as reducing agent with kanamycin A and neomycin as stabilizing agents. <sup>16</sup> They prepared larger nanoparticles with agglomeration.

In the present study, the synthesis and characterization of monodispersed small gold nanoparticles using fruit extract of *Ananas comosus* has been described. Here the size and aggregation of the nanoparticles were controlled without any additional stabilizing agents. The sensing activity of gold nanoparticles obtained by this method has been also described.

#### 2. Experimental Techniques

#### 2. 1. Materials and Methods

Ananas comosus fruit was collected from local supermarket in Kodaikanal, Tamilnadu, India. Chloroauric acid and various heavy metals were obtained from Sigma Aldrich Chemicals. All glasswares were properly washed with distilled water and dried in hot air oven before use.

#### 2. 2. Preparation of Ananas Comosus Extract

Fully riped *Ananas comosus* fruit weighing 100 g cut into fine pieces and were crushed into 100 ml distilled water in a mixer grinder for extraction. The extract was then separated by centrifugation at 1000 rpm for 10 min to remove insoluble fractions and macromolecules. Then the extract obtained was filtered and finally a light yellow extract was collected for further experiments.

#### 2. 3. Synthesis of Gold Nanoparticles

For the synthesis of gold nanoparticles, 5ml of *Ananas comosus* extract was added to aqueous solution of HAuCl<sub>4</sub>(3 mM) and stirred continuously for 5min at room temperature. Upon addition of fruit extract, the color of the solution gradually changes from light pink to charac-

teristic dark ruby red upon completion of reaction of the gold colloid (g1). Similarly by adding 10 and 15 ml of fruit extract two more set of samples henceforth called (g2) and (g3) respectively were prepared. UV-visible spectra of these solutions were recorded. Then the solutions were dried. The dried powders were characterized by X- ray diffraction (XRD), Fourier Transform Infrared Radiation (FTIR), Transmission Electron Microscope (TEM) and Energy Dispersive X-ray Spectroscopy (EDX).

### 2. 4. Characterization Methods and Instruments

The absorption spectra of the prepared nanoparticles were measured using a Shimadzu spectrophotometer (UV 1700) in 300–800 nm range. X- Ray Diffraction analysis of the prepared nanoparticles was done using PANalytical X'pert – PRO diffractometer with Cu Kα radiation operated at 40 kV/30 mA. FTIR measurements were obtained on a Nexus 670 FTIR instrument with the sample as KBr pellets. Transmission Electron Microscopic (TEM) analysis was done using a JEOL JEM 2100 High Resolution Transmission Electron Microscope equipped with an EDX attachment, operating at 200kV.

#### 3. Results and Discussion

#### 3. 1. UV-visible Studies

Noble metals are known to exhibit unique optical properties due to the property of SPR which is the collective oscillation of the conduction electrons in resonance with the wavelength of irradiated light. In the present

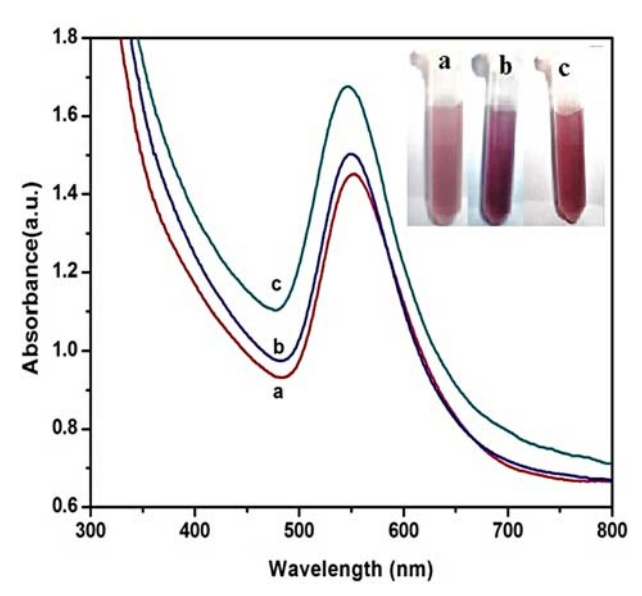


**Figure 1.** Optical absorption spectra of AuNPs at different concentration of *A. comosus* fruit extract (inset: colour changes of the prepared AuNPs) (a, b and c vs 5, 10 and 15 ml respectively).

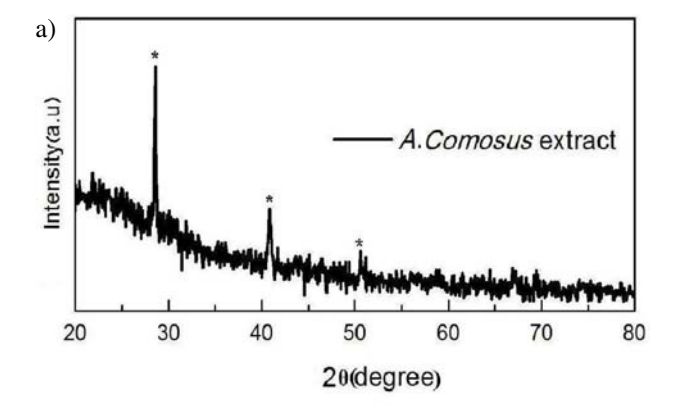
study the formation of gold nanoparticles was initially conformed using UV-Visible spectroscopy by measuring Surface Plasmon Resonance (SPR) peaks. Gold nanoparticles exhibit plasmon absorption bands that depend on their size and shape. Fig. 1 shows the absorption spectra obtained for gold nanoparticles with different concentration of fruit extract. The colour variation of the obtained gold nanoparticles for different concentration of Ananas comosus fruit extract has been shown in Fig. 1(inset). These characteristic color variations are due to the excitation of the surface plasmon resonance in the metal nanoparticles. As the concentration of fruit extract increases, an fwhm value decreased from 105 nm to 94 nm and blue shift observed from 550 to 544 nm in the reaction medium, indicating the formation of small nanoparticles.

As the particles decrease in size, the absorption peak usually shifts toward the blue wavelengths caused by the donation of electrons to the particles. It has been well established that the maximum wavelength of nanoparticles strongly depends on size, shape, state of aggregation and the dielectric environment. This directly corresponds to a shift of the absorption peak, whereby small gold particle sizes will cause an absorption peak shift to smaller wavelengths, higher frequency and energies.<sup>17</sup> The observed symmetric nature of the SPR indicates the formation of spherical nanoparticles. As the concentration of the extract increases more number of citric, malic and ascorbic acids are available to reduce gold ion and forms large number of very small nanoparticles gives rise to sharp, intense and blue shifted SPR. It was further confirmed by the TEM images shown in Fig. 4 and 5. The symmetric nature of the SPR and the absence of peaks in the longer wavelength region indicate the absence of nanoparticle aggregation. Ascorbate, malate and citrate ions in the fruit extract introduce the negative charge onto the particle surface and thus preventing the particles from aggregation. Thus from the results it can be concluded that the concentration of fruit extract plays an important role in the formation of gold nanoparticles. The obtained nanoparticles were stabilized by physical adsorption of excess negatively charged citrate, malate and ascorbate ions in the solution medium, and thus a repulsive force worked along particles electrostatically and preventing them from aggregation.

#### 3. 2. XRD Studies

The crystalline structure and phase purity of the prepared gold nanoparticles were confirmed with X-ray diffraction (XRD) analysis. Fig. 2(a) shows the XRD pattern for the dried powder of *Ananas comosus*. Three diffraction peaks were observed at 28.5°, 40.8° and 50.9° signify the presence of ascorbic acid (JCPDS 22-1560), citric acid (JCPDS 22-1568) and malic acid (JCPDS 23-1631) in the *Ananas comosus* extract.

Fig. 2(b) shows the XRD pattern for g1 and g3. The broad diffraction peaks were observed at 38.2°, 44.1°,



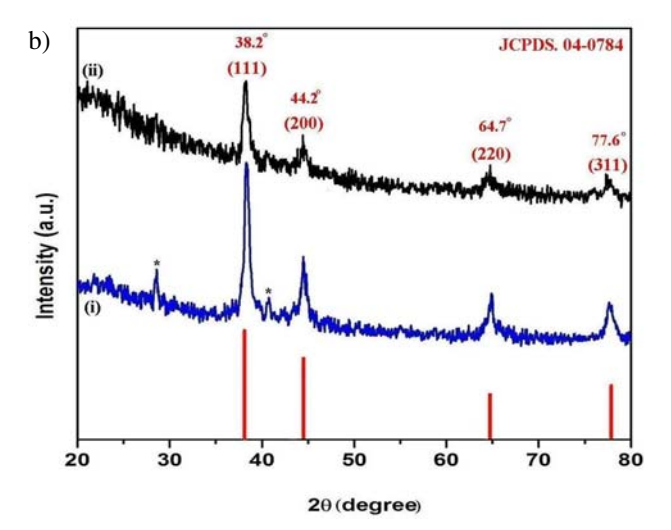


**Figure 2.** X-ray diffraction pattern of (a) *A.comosus* fruit extract and (b) AuNPs (i) g1 and (ii) g3.

 $64.8^{\circ}$  and  $77.6^{\circ}$  in the 20 range and they corresponding to (111), (200), (220) and (311) Bragg's reflections based on the FCC structure of gold nanoparticles with space group of Fm-3m (JCPDS: 04-0784). No peaks of crystallographic impurities in the sample have been found. Generally, the breadth of a specific phase of material is directly proportional to the mean crystallite size of that material. The obtained broader peaks with increasing fruit extract concentration indicating smaller particle size. The XRD line width can be used to estimate the size of the particle by using the Debye-Scherrer formula as D =  $k\lambda\beta$  cos $\theta$  where D is the particle size (nm), k is a constant equal to 0.94,  $\lambda$  is the wavelength of X-ray radiation (1.5406 Å),  $\beta$  is the full-width at half maximum (FWHM) of the peak (in radians) and  $2\theta$  is the Bragg angle (degree). The average particle size, lattice constant, cell volume, surface area to volume (SA: V) ratio, specific surface area (SSA) and Crystallinity index were calculated and tabulated Table.1.

The calculated average particle size for both g1 and g3 indicates that the particle size decreased with the concentration of the fruit extract increased. The calculated lattice constant values are very close to the standard data

Prepared AgNPs	Particle Size (nm)	Lattice constant ( Å)	Cell volume ( ų)	SSA (m²/g)	SA:V ratio	Crystallinity index Icry
g1	16	4.0529	66.57	18.46	0.35	~1.0625
g3	7	4.0815	67.99	40.64	0.78	~0.714

Table.1. The average particle size, lattice constant, cell volume, surface area to volume (SA: V) ratio, specific surface area (SSA) and crystallinity index of the prepared nanoparticles.

(JCPDS File no. 04-0784) and the sample exhibit smaller cell volumes that of bulk. As shown in Table. 1, the observed values of both specific surface area (SSA) and SA:V ratios were increased with decreasing particle size. The SSA has a particular importance in reactivity. It gives the rate at which the reaction will proceed. Because of the large number of atoms available in the reaction medium (g3) makes the reaction faster and hence make them more suitable for broad kind of applications. Crystallinity was evaluated by comparing the crystalline size obtained by XRD to TEM particle size determination. The calculated values of crystallinity index were close to one which indicates the monocrystalline nature of g1 and g3.

#### 3. 3. FTIR Studies

FTIR analysis was carried out to identify the chemical change of the functional groups involved in bioreduction. Fig.3(a) shows the FTIR spectrum of the *Ananas comosus* fruit extract, shows prominent bands at 3417, 2924, 1640, 1019 and 801 cm<sup>-1</sup> in the 4000 –500 cm<sup>-1</sup> region. These peaks are assigned to O-H stretching, C+C ring stretching, C-O-C stretching and C-C ring stretching of ascorbic acid, respectively. Fig. 3(b) shows that the FTIR spectrum of g3. The peak at 3417 cm<sup>-1</sup> was also due to the OH stretching of citric and malic acid. 19,20

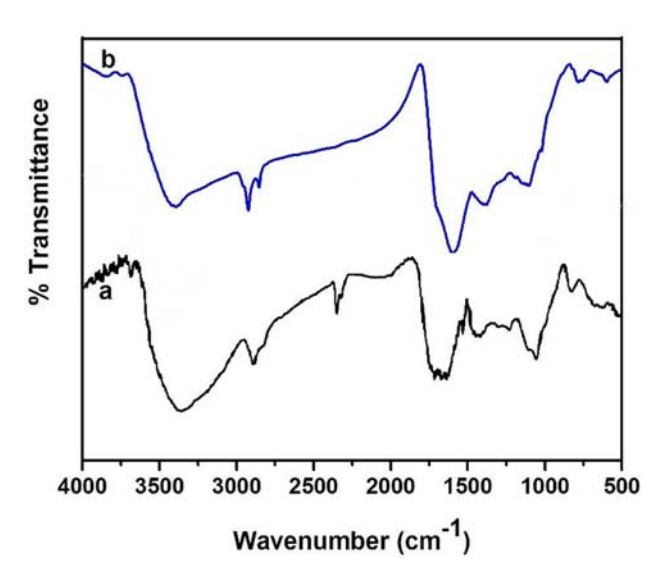


Figure 3. FTIR spectra of (a) A.comosus fruit extract and (b) g3.

An interesting peak observed at 2369 cm<sup>-1</sup> in the spectrum of extract was assigned to NH<sup>-</sup> stretching of amines. This vibrational mode was completely reduced in the spectrum of g3. It may the presence of bromelain in the extract. Bromelain is a protein which functions as an enzyme known as proteolytic enzymes. These enzymes have the ability to separate all important peptide bonds. This possibly leads to the absence of this vibrational mode during the synthesis of gold nanoparticles (g3). The interesting peak at 1640 cm<sup>-1</sup> in the spectrum of extract was assigned to C=C ring stretching of vitamin C, OCO asymmetric stretching of malic acid and C=O stretching of citric acid, was appeared at a sharp peak at 1601 cm<sup>-1</sup> in the spectrum of g3.

Another interesting broad peak observed at 1414 cm<sup>-1</sup> in the spectrum of extract was show at a symmetric peak at 1390 cm<sup>-1</sup> in the spectrum of g3, was due to OCO symmetric stretching of malic acid, COH deformation of citric acid and CH<sub>2</sub> wagging of ascorbic acid. Similarly, the symmetric peak observed at 1115 cm<sup>-1</sup> was due to C-O-C stretching of ascorbic acid and C-C stretching of malic and citric acid. This indicates that the carboxylic acid groups present in the *Ananas Comosus* fruit extract was responsible for reduction of AuNPs.

#### 3. 4. TEM Studies

The TEM images of the g1 and g3 were shown in Fig. 4 and 5 respectively. The prepared nanoparticles exhibit size dependent morphology. At the TEM image of g1, monodispersed and spherical nanoparticles of average size of 17 nm with diameter ranging from 13 nm to 26 nm (Fig.4). The TEM image of g3, synthesized by higher fruit extract concentration showing the presence of monodispersed spherical nanoparticles of average size of 7 nm ranging from 3 to 15 nm size (Fig. 5). Here, most of the particles observed in the range of 4 nm to 8 nm. As the concentration of fruit extract increases large number of citrate, malate and ascorbate ions are available to reduce gold ion and forms small nanoparticles. The smaller size of g3 was also due to their high specific surface area and its monocrystalline nature. More number of nanoparticles observed in TEM images of g3 in comparison to g1. In both cases, the observed nanoparticles were spherical and homogeneous distribution, which was confirmed from the symmetric nature of SPR shown in Fig. 1(a). Strong interaction between biomolecules in the fruit extract and sur-

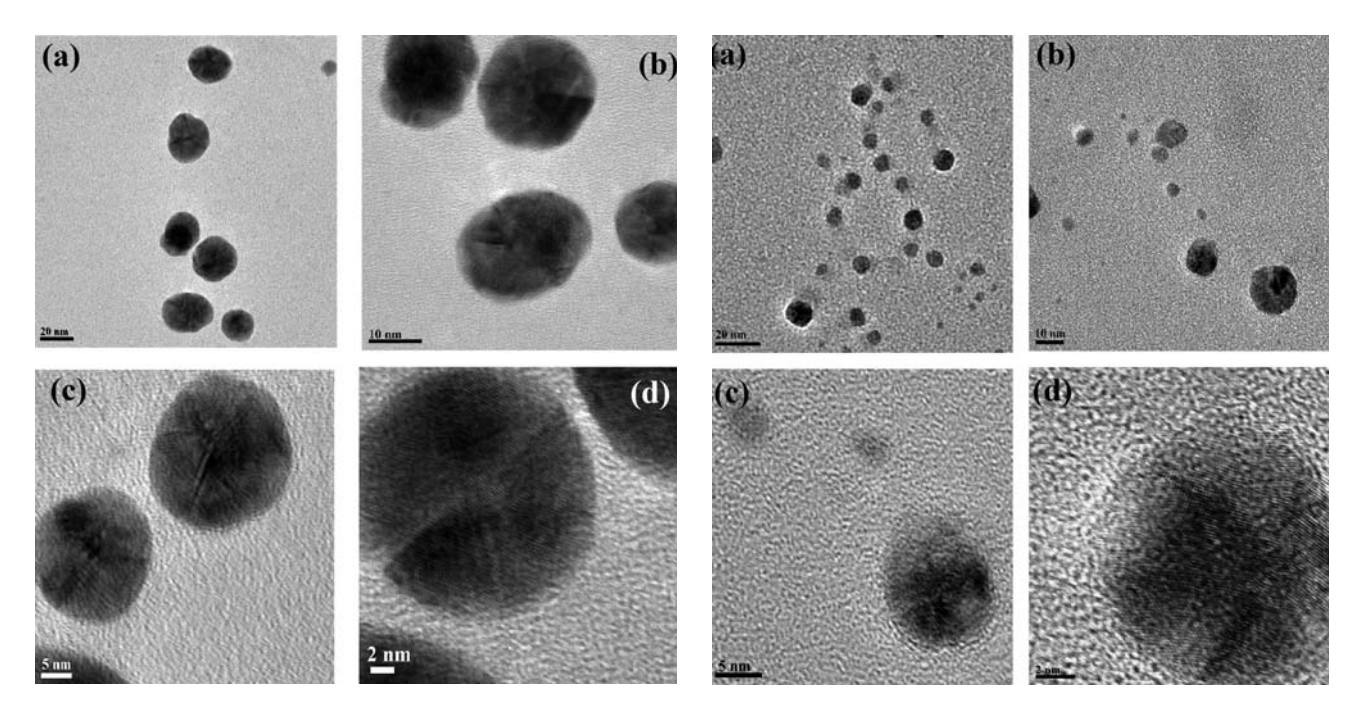


Figure 4. TEM micrograph of the g1.

Figure 5. TEM micrograph of the g3.

face of nanoparticles was sufficient to the formation of spherical nanoparticles preventing them from sintering.

At lower concentration of fruit extract the citric, ascorbic and malic acid present in fruit extract was insufficient to reduce gold ion, indicating larger size particle. The twined particles observed in Fig. 4(c), 4(d), 5(c) and 5(d) were identified by showing brightness in part of the particles as compared to the other parts. Generally, twinning, the planar defect is observed for face-centered cubic (fcc) structured metallic nanocrystals. Sharing of a common crystallographic plane by two subgrains gives rise to twinning. Face-centered cubic (fcc) structured metallic nanostructures have a tendency to nucleate and grow into twinned particles with their surfaces bounded by lowest

energy facets (111)<sup>21</sup>. The formation of gold was further confirmed by the analysis of the energy dispersive spectroscopy shown in Fig. 6.

#### 3. 5. Sensing Activity

Sensing is one of the important applications of nanoparticles. Nanoparticle-based optical surface sensors have received much attention due to their faster response and better resolutions. The interaction between natural biomolecules and the surface of the inorganic nanoparticles paves the way for development of sensing system. The interaction of prepared AuNPs with various alkali metal (Li<sup>+</sup>, K<sup>+</sup>, Fe<sup>3+</sup>) and transition metal ions (Ni<sup>2+</sup>, Mn<sup>2+</sup>, Cu<sup>4+</sup>,

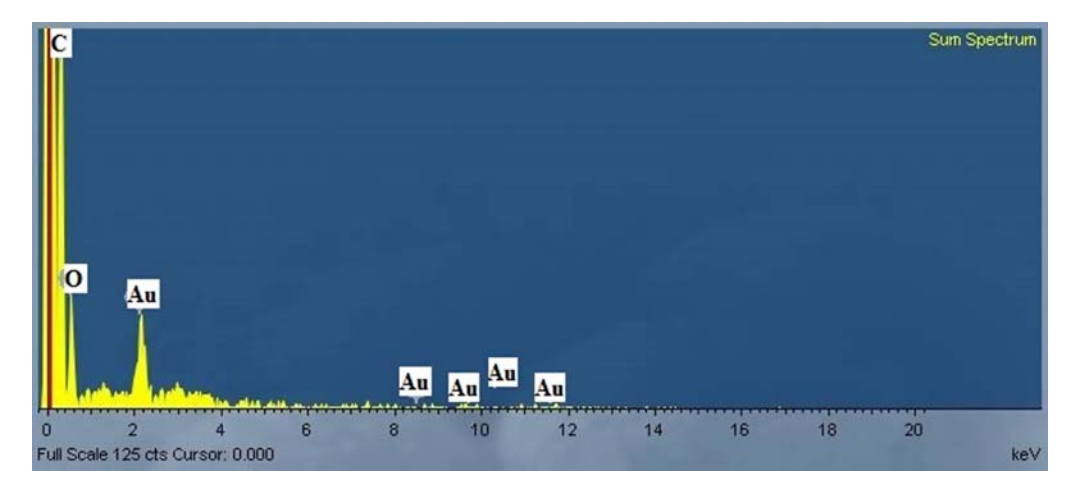
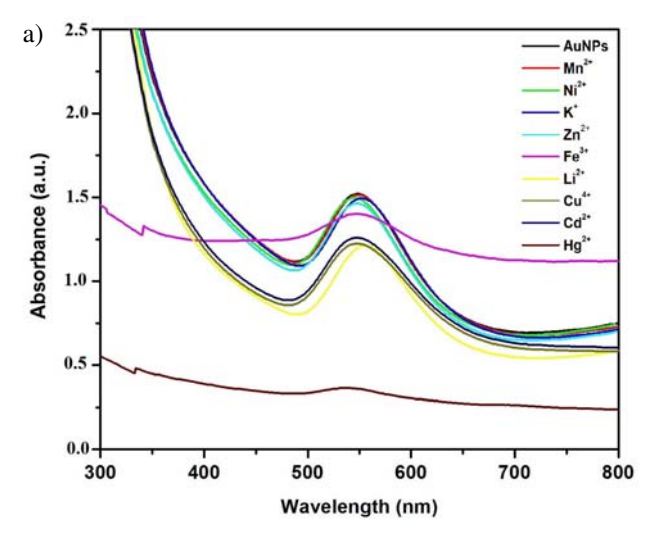
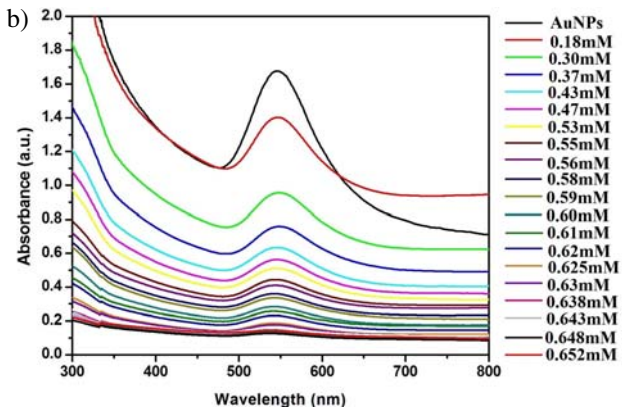


Figure 6. EDX graph of g3.

Zn<sup>2+</sup>, Hg<sup>2+</sup>, Cd<sup>2+</sup>) was examined by adding 1ml of (3mM) salts of these metals into the 2 ml of AuNPs by drop by drop and stirred for 5 min. UV-vis spectra (Fig.6 (a)) of AuNPs were taken immediately after addition of metal ions, after 5 min of interaction. It was observed that except Hg<sup>2+</sup> no other metal ions exhibited a colour change. UV-vis spectra of these heavy metals interacted with Au-NPs were shown in Fig.7 (a). It was observed that the intensity of the SPR bands get reduced for all metal ions as compared to that of the AuNPs. Only mercury got almost quenching of the SPR peak among all the metals, including alkali metal (Li+, K+, Fe3+) and transition metal ions  $(Ni^{2+}, Mn^{2+}, Cu^{4+}, Zn^{2+}, Hg^{2+}, Cd^{2+})$ . It was also observed that for Hg<sup>2+</sup> gave fading of pale pink colour, indicating the prepared AuNPs were sensitive and selective towards  $Hg^{2+}$ .

The sensitivity of this method was measured by adding various concentration of aqueous solution of Hg<sup>2+</sup> ions to the aqueous AuNPs (5 ml) at room temperature. With the increase of Hg<sup>2+</sup> ions, the color sequentially changed from purple to colorless. The addition of 0.188 mM to 0.653mM Hg<sup>2+</sup> to the AuNPs solution causes color changes from light purple to colorless were observed shown in Fig. 7 (b) (inset). The UV-vis spectrum correspondingly recorded and shown in Fig. 7(b). With increasing the concentration of Hg<sup>2+</sup> ion to the AuNPs causes immediate reduction in the intensity of surface plasmon peak at 544 nm. This could be accounted for the slight blue shift of the SPR band of gold nanoparticles. It shows absorbance strength decreases gradually by increasing the concentration of Hg<sup>2+</sup> ion. With increasing Hg<sup>2+</sup> ion concentration, blue shift of the SPR peak was also obtained. When Hg<sup>2+</sup> ion added to the prepared nanoparticles, Hg<sup>2+</sup> ions interact with the biomolecules (carboxylic acid groups) in the Ananas comosus fruit extract on the surface of the nanoparticles form bonds among nanoparticles with Hg<sup>2+</sup> ions performing as link for binding sites of biomolecules and eliminating it away from the surface of the nanoparticle surface, in that way aggregation of nanoparticles had taken place. This could be accounted for the slight blue shift of the SPR band of gold nanoparticles. There was no SPR peak was observed after the addition of 0.653 mM Hg<sup>2+</sup>, suggesting the concentration of Hg<sup>2+</sup> was limited to 0.653 mM. So The linear variation of absorbance  $(\Delta A)$  changes and the concentration of Hg<sup>2+</sup> over the range from 0.188 mM to 0.653mM shown in Fig. 7(c). This plot can be fit by a linear equation y = 1.527x-1.0633,  $R^2$ = 0.9889. The sensitivity of the system towards analyte concentration was found to be 1.5273/mM is measured from the plot of absorbance ( $\Delta A$ ) versus concentration of Hg<sup>2+</sup>. The limit of detection was estimated by defined as the following formula of  $C_L = 3S_B/m$ , where  $C_L S_B$  and m are the limit of detection, standard deviation of the sample, and the slope of the calibration curve, respectively. It was found to be 0.1198 mM. Applications of nanoparticle sensors by the aggregation of small particles were useful





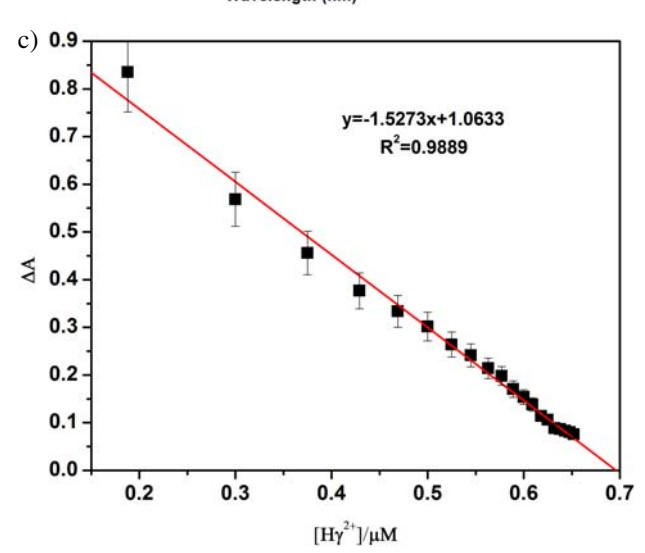


**Figure. 7.** (a) UV-vis absorption spectrum and photographs (inset) of AuNPs with different heavy metal ions, (b) UV-vis absorption spectrum of AuNPs solution upon addition of  $Hg^{2+}$  ions (0.188 mM to 0.653mM) and (c) plot of absorbance ( $\Delta A$ ) intensity at 544 nm versus  $Hg^{2+}$  ions concentration.

because aggregates with multiple particles yield large enhancements due to the enormous electromagnetic field that coherently interfere at the junction site between the

particles. This mercury sensor based on surface plasmon optical sensor can be used in environmental monitoring especially in water purification.

#### 4. Conclusion

The present simple study was designed to slow reduction of chloroauric acid using fruit extract of Ananas comosus as reducing agent. This green synthesis method has formed monodispersed spherical gold nanoparticles with average size of 7 nm. The prepared nanoparticles were characterized by UV-visible, Fourier transform infrared spectroscopy (FTIR), transmission electron microscopy (TEM) and energy dispersive spectroscopy (EDS) technique to identify the size, shape of nanoparticles and biomolecules act as reducing agents. FTIR measurements show that carboxylic acid groups present in Ananas comosus fruit extract was used as reducing agent. The prepared gold nanoparticles were stable for one month without aggregation. The surface plasmon resonance of prepared gold nanoparticles was confirmed by UV-visible spectral analysis. As the concentration of *Ananas comosus* fruit extract increases, absorption spectra shows blue shift with decreasing particle size. The prepared AuNPs were sensitive and selective towards Hg2+. This mercury sensor based on surface plasmon optical sensor can be used in water analysis by detecting the concentration of Hg<sup>2+</sup> ions.

#### 5. Acknowledgements

The authors are thankful to DST-CURIE New Delhi, UGC-DAE CSR Indore for financial assistance.

#### 6. References

- M. A. Anderson, F. M. M. Morel, *Limnol. Oceanogr.* 1978, 23, 283–295. https://doi.org/10.4319/lo.1978.23.2.0283
- F. A. Cotton, G. Wilkinson, C. A. Murillo, M. Bochmann, Advanced Inorganic Chemistry, 6th ed., John Wiley & Sons, New York, 1999.
- T. W. Clarkson, L. Magos, G. J. Myers, N. Engl. J. Med. 2003, 349, 1731–1737. https://doi.org/10.1056/NEJMra022471

- 4. Y. Wang, F. Yang, X. Yang, *Biosens. Bioelectron.* **2010**, *25*, 1994–1998. https://doi.org/10.1016/j.bios.2010.01.014
- M. Umadevi, S. Shalini, M. R. Bindhu, Adv. Nat. Sci. Nanosci. Nanotechnol. 2012, 3 025008, 1–6.
- M. Umadevi, M. R. Bindhu, V. Sathe *J. Mater. Sci. Technol.* 2013, 29, 317–322. https://doi.org/10.1016/j.jmst.2013.02.002
- 7. M. R. Bindhu, M. Umadevi, Spectrochim. Acta A, 2015, 135,
- 373–378. https://doi.org/10.1016/j.saa.2014.07.045 8. M. R. Bindhu, M. Umadevi, *Spectrochim. Acta A*, **2013**, *101*, 184–190. https://doi.org/10.1016/j.saa.2012.09.031
- M. R. Bindhu, V. G. Sathe, M. Umadevi, Spectrochim Acta A, 2013, 11, 5409–415
- V. Armendariz, I. Herrera, J. R. Peralta-Videa, M. Jose-Yacaman, H. Troiani, P. Santiago, J. L. Gardea-Torresdey, *J. Nanopart. Res.* 2004, 6, 377–382. https://doi.org/10.1007/s11051-004-0741-4
- M.R. Bindhu, P.Vijaya Rekha, T. Umamaheswari, M.Umadevi, *Mater. Lett.* **2014**, *131*, 194–197. https://doi.org/10.1016/j.matlet.2014.05.172
- 12. J. L. Collins, The Pineapple, Interscience Publishers Inc New York. (1960) 250.
- E. K. Nelson, J. Am. Chem. Soc. 1925, 47, 1177–1179. https://doi.org/10.1021/ja01681a039
- 14. X. Hu, M. Zhao, H. Huang, Water Environ. Res. 2010, 8, 2733–741.
- X. Hu, M. Zhao, G. Song, H. Huang, *Environ Technol. 32*, 2011, 739–746. https://doi.org/10.1080/09593330.2010.510853
- V. Santosh Nalage, V. Sidhanath Bhosale, V. Sheshanath Bhosale, ONJ 2011 5, 78–82.
- S. L. Smitha, K. M. Nissamudeen, D. Philip, K. G. Gopchandran, *Spectrochim. Acta A* 2008 *71*, 186–190. https://doi.org/10.1016/j.saa.2007.12.002
- C. Y. Panicker, H. T. Varghese, D. Philip, *Spectrochim. Acta A*, **2006** *65*, 802–804. https://doi.org/10.1016/j.saa.2005.12.044
- P. Tarakeshwar, S. Manogaran, Spectrochim. Acta A 1994 50, 2327–2343. https://doi.org/10.1016/0584-8539(94)E0017-5
- J. L. Castro, M. R. López-Ramýírez, J. F. Arenas, J. C. Otero, *Vib. Spectrosc.* **2005** *39*, 240–243. https://doi.org/10.1016/j.vibspec.2005.04.007
- 21. J. G. Allpress, J. V. Sanders, *Surf. Sci.* **1967**, *7*,1–25. https://doi.org/10.1016/0039-6028(67)90062-3

#### Povzetek

Nanodelce zlata smo pripravili z uporabo *Ananas comosus* kot reducirnega reagenta. UV-Vis spektri kažejo površinsko resonančni plazmonski (SPR) vrh pri 544 nm. Z meritvami s presevnim elektronskim mikroskopom (TEM) pa smo prikazali sintezo monodispergiranih sferičnih nanodelcev s povprečno velikostjo 7 nm. Kristalna narava nanodelcev je razvidna iz TEM slik in vrhov, določenih z rentgensko praškovno difrakcijo (XRD). FTIR spektroskopija kaže na prisotnost biomolekul, ki so odgovorne za redukcijo in ločevanje pripravljenih nanodelcev zlata. Za določanje živega srebra predlagamo selektivno in občutljivo metodo, ki temelji na osnovi SPR sprememb nanodelcev zlata. Takšen senzor bi lahko uporabljali pri analizi voda